PROTEINS: Structure, Function, and Genetics 44:244–254 (2001)

Denatured Collapsed States in Protein Folding: Example of Apomyoglobin

Olga Tcherkasskaya[1†] **and Vladimir N. Uversky**[2,3]
[1]*Laboratory of Experimental and Computational Biology, National Cancer Institute, National Institutes of Health, Bethesda, Maryland*
[2]*Department of Chemistry and Biochemistry, University of California, Santa Cruz, California*
[3]*Institute for Biological Instrumentation, RAS, Pushchino, Moscow Region, Russia*

ABSTRACT **Experimental approaches, including circular dichroism, small angle X-ray scattering, steady-state fluorescence, and fluorescence energy transfer, were applied to study the 3D-structure of apomyolgobin in different conformational states. These included the native and molten globules, along with either less ordered conformations induced by the addition of anions or completely unfolded states. The results show that the partially folded forms of apomyoglobin stabilized by KCl and/or Na_2SO_4 under unfolding conditions (pH 2) exhibit a significant amount of secondary structure (circular dichroism), low packing density of protein molecules (SAXS), and native-like dimensions of the AGH core (fluorescence energy transfer). This finding indicates that a native-like tertiary fold of the polypeptide chain, i.e., the spatial organization of secondary structure elements, most likely emerges prior to the formation of the molten globule state. Proteins 2001;44:244–254.** © 2001 Wiley-Liss, Inc.*

Key words: apomyoglobin; fluorescence energy transfer; denatured collapsed state; molten globule state; protein folding.

INTRODUCTION

It is well accepted nowadays that the folding of globular proteins is a multistage process, which includes the formation of several intermediate conformational states. Though a number of intermediates have been found both in kinetic and equilibrium studies,[1] only two of them, namely, the molten globule and its precursor, have been analyzed thoroughly.[1–4] Structural studies of the molten globule (MG) states of a variety of proteins have revealed features that appear to be general.[1,5–9] The emerging consensus is that this folding intermediate exhibits a high content of secondary structure, considerable compactness, nonspecific tertiary structure, and significant structural flexibility. These characteristics often are used to define a general MG state, which is structurally and thermodynamically distinct from both the native and the fully unfolded states. Much less is known regarding the recently revealed premolten globule (PMG) state.[2–4] Altogether, proteins in the PMG state exhibit a lack of unique tertiary structure but may have a significant amount of ordered secondary structure. Pre-molten globules were found to be rather compact, but their molecular dimensions are larger than for molten globules. There is no experimental evidence that proteins in the PMG state have a tightly packed globular core. It is possible, however, that some elements of the secondary structure are packed natively even at this stage of folding.[3] Further, the PMG state is separated by sharp transitions from both the molten globule and the completely unfolded (U) states.[2–4] Though new data on folding intermediates are being reported more frequently, all the mysteries of protein folding have not yet been resolved. For example, the most important question remains unanswered: When during the process of protein folding does the native tertiary fold emerge?

Over the last decade, several model systems have found widespread use in the protein folding field. One such protein is apomyoglobin (apoMb), i.e., heme-free myoglobin (Fig. 1). The structure of native apoMb is very similar to that of native holomyoglobin[10–14] and the molecular dimensions of the native apo- and holo-forms differ by less than 12 %. Apomyoglobin is a small (153 residues), α-helical protein, which has been intensively studied by a plethora of biochemical and biophysical techniques.[15] The protein undergoes structural transformations upon decrease of pH and reaches the molten globule state at pH 4.2 and the acid-unfolded state at pH 2 and low ionic strength.[10,16] Experimental conditions to populate a particular equilibrium state have been worked out[17] and the biophysical characterization of these states has been reported.[15] As for the 3D-structure of the molten globule intermediate, the combination of deuterium exchange and 2D-NMR has revealed that the native A, G, H helices of apoMb become stable at an early stage of protein folding[18] and are relatively stable in the equilibrium MG state.[10] Multidimensional NMR spectroscopy defined the backbone conformation of residues in the MG state, suggesting localization and high probability of these helices.[19] Regarding the tertiary structure, fluorescence experiments dem-

Abbreviations: ApoMb, apomyoglobin; CD, circular dichroism; MG, molten globule; PMG, pre-molten globule; SAXS, small-angle X-ray scattering; SDS, sodium dodecyl sulfate; Trp, tryptophan; Tyr, tyrosine.

† Correspondence to: Olga Tcherkasskaya, Laboratory of Experimental and Computational Biology, National Cancer Institute, National Institutes of Health, Bethesda, MD 20892.
E-mail: tcherkasskaya@nih.gov.

Received 4 January 2001; Accepted 20 April 2001

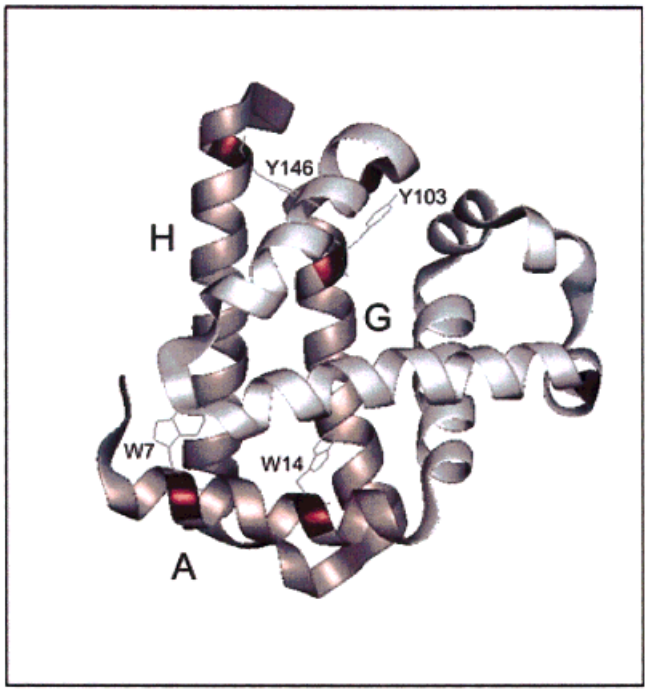

Fig. 1. Ribbon representation of native apomyoglobin showing tryptophan residues W7 and W14 residing on the A-helix and the tyrosine residues Y103 and Y146 located on the G- and H-helices, respectively. The native A, G, and H helices are formed early in protein folding and are relatively stable in the equilibrium molten globule state.

onstrated that the AGH complex in the MG state constitutes a native-like subdomain.[20,21]

Recently, it was found that the structure of acid-unfolded apoMb could be varied by the nature of anions added to solution.[9,22–25] All the anion-induced forms studied so far exhibit smaller amounts of rigid tertiary structure than does native protein, and differ noticeably in the extent of secondary structure, molecular size, and conformational stability.[22,23] It has been assumed that these partially folded forms might correspond to discrete conformational states of the apoMb folding. Yet the structure of these nonnative forms still remains unclear. In this regard, we proposed a method to probe the 3D-structure of nonnative proteins, based on measurements of average distances between groups of the protein by means of direct energy transfer technique.[20] For these experiments, Tyr residues are to be modified by reaction with tetranitromethane to convert to a nitro-form, Tyr(NO_2). This results in substantial changes of Tyr spectral properties, and renders this residue as an acceptor for Trp electronic energy.[20,26–28] The extent of decrease of Trp fluorescence in the presence of nitro-Tyr provides a measure of average distance R_{DA} between these residues.

Horse myoglobin contains Trp7 and Trp14 in the middle of the A-helix, along with Tyr103 at the beginning of the G-helix and Tyr146 at the end of the H-helix (Fig. 1). Both tyrosine residues can be converted successively into the nitro-form.[20] Comparison of Trp fluorescence in unmodified and modified samples permits the evaluation of the distances from Trp residues to individual Tyr residues, i.e., the distances between identified points on the protein. Employing the energy transfer method to a variety of nonnative forms of horse apoMb revealed that the AGH helical complex, being the most structured part of the molten globule, exists also in nonnative forms stabilized by NaTCA, NaTFA, $NaClO_4$.[28] Thus, all partially folded forms of apoMb so far known share this common feature of native structure. The present study focuses on the nonnative forms of apoMb, which exhibit the most expanded conformations. In particular, the equilibrium refolding of acid-unfolded apoMb was induced by the presence of KCl and/or Na_2SO_4 and was monitored by circular dichroism, small-angle X-ray scattering, steady state fluorescence, and fluorescence energy transfer. We demonstrate that it is possible to observe partially structured conformations of apoMb, which exhibit a significant amount of secondary structure, the low packing density of a protein molecule, and the native-like dimensions of the AGH core.

MATERIALS AND METHODS

Preparation of Apomyoglobin

Horse myoglobin (isolated from heart muscle) was purchased from Sigma (St. Louis, MO). The heme was removed by 2-butanone extraction[29] followed by gel chromatography on Sephadex G-25 (PD-10 columns, Pharmacia, Piscataway, NJ). The apo-protein was extensively dialyzed against water at 4°C and lyophilized for storage. Contamination of the apo-protein by myoglobin was assessed spectrophotometrically, and no significant absorption was observed in the Soret region. Homogeneity of the apoproteins was verified by SDS-polyacrylamide gel electrophoresis;[30] a single band was observed for each sample. Protein concentration was estimated by absorbance at 280 nm with a Hewlett-Packard 8452A diode array spectrophotometer. The molar extinction at 280 nm was calculated from the tryptophan and tyrosine composition and the standard values of 5,690 and 1,280 $M^{-1}(cm^{-1}$ reported for those amino acids.[31]

Chemicals and Solutions

All reagents were reagent grade or better. Ultra-pure KCl and/or Na_2SO_4 was purchased from ICN (Irvine, CA) and used without further purification. Most experiments were carried out at 23°C in a 10 mM sodium acetate, 10 mM sodium phosphate buffer mixture. In addition, the experiments were performed in deionized water in salt free solutions and/or in the presence of 30 mM NaCl meant to stabilize the MG state.[16] This variation in conditions led to no changes in experimental parameters. The native and molten globule states were studied at pH 6.5 and 4.2, respectively.[17] The unfolded state was achieved by dissolving salt free apoMb in 10 mM HCl (pH 2). To prepare the nonnative forms of apoMb induced by the presence of KCl or Na_2SO_4, we followed the procedure reported previously.[22,23] The appropriate salt was dissolved in 10 mM HCl (pH 2) and thereafter mixed with the unfolded apoMb solution to prepare the desired anion concentrations. Each sample was equilibrated for 20 min prior to measurements. This time is sufficient for completion of the anion-

induced refolding.[22] No changes in experimental data were observed after further 24 h. The pH was measured using a Radiometer PHM83. The refractive index was measured with a AO Abbe refractometer.

Small-Angle X-Ray Scattering Experiments

Small-angle X-ray scattering (SAXS) measurements were carried out on a Beam Line 4-2 at Stanford Synchrotron Radiation Laboratory essentially as described.[32] X-ray energy was selected at 8,980 eV (Cu edge) by a pair of Mo/B_4C multilayer monochromators.[33] A linear, position-sensitive, proportional counter filled with 80% Xe and 20% CO_2 gas mixture was used to record a scattering pattern. Each pattern was normalized by incident X-ray intensity measured with a short length ion chamber placed prior to the sample. The sample-to-detector distance was calibrated at 230 cm using a cholesterol myristate standard. Experiments were carried out for protein concentrations covering the range 5–20 μM. No changes in recovered parameters were observed, demonstrating that no significant aggregation is present. Since we used extremely low protein concentrations, the measurement time was about 60 min. To avoid radiation damage to the sample, the protein solution was continuously passed through a 1.3-mm path-length flow cell with 25-μm mica windows. Background signal was recorded before and after each measurement and the averaged value was used in the data analysis.

Overall, X-ray scattering by proteins in solution is sensitive to spatial fluctuations in electron density. Scattering at the smallest angles yields the radius of gyration, R_g, which in conjunction with the protein molecular weight, provides a measure of the compactness of molecules.[34] In particular, the radius of gyration can be recovered by the "Guinier plot," which assumes that low-angle scattering can be described by the following function:

$$\ln I(q) = \ln I(0) - \frac{R_g^2}{3} q^2 \qquad (1)$$

In eq 1, the scattered intensity is denoted as $I(q)$; $= \frac{4\pi sin\theta}{\lambda}$ is the magnitude of the difference between the wave propagation vectors for incident and scattered radiation; λ is the X-ray wavelength, 1.488 Å; and 2θ is the scattering angle. The forward scattering amplitude $I(0)$ relates to the number of scatterers in solution, n; the difference in electron densities of the scatterer and the solvent, ρ_c; and to the volume V of the scatterers, i.e., $I(0) \sim n \cdot \rho_c^2 \cdot V^2$. Equation 1 was fitted to the raw data, using the commercial software implemented in the KaleidaGraph (Synergy Software, Reading, PA). The range of validity of the Guinier-approximation included the q values from 0.28 to 0.45 nm^{-1}. For each sample, the radius of gyration (the average of three independent measurements) was calculated and used in further analysis. Based on the results of the replicates, we anticipate uncertainty in R_g to be below 5%. Since a large number of macromolecular geometries can appear in a particular conformational state, the scattering experiments report the mean square radius of gyration $\langle R_g^2 \rangle$. This parameter of the conformational distribution is most influenced by large species. Additional structural information was obtained from scattering at larger angles, which reflects electron density correlations on length scales shorter than R_g. Specifically, employing the Kratky plots, $I(q) \cdot q^2$ vs. q, allows one to distinguish between random coil and compact conformations (see below).

Circular Dichroism Measurements

Circular dichroism (CD) measurements were carried on an AVIV 62DS spectrophotometer (Lakewood, NJ) equipped with a temperature-controlled cell holder. The spectropolarimeter was calibrated with (+)-10-camphorsulphonic acid prior to measurements. Spectra were recorded over 190–250 nm in 0.5-nm steps for 10 μM protein samples in a 0.1-cm cell (bandwidth of 1.5 nm, averaging time of 15 sec). Each spectrum (averaged over 10 scans) was corrected for the appropriate solvent-blank. Raw data were expressed as molar ellipticity[35] in units of degree · $cm^2 \cdot dmol^{-1}$.

Steady-State Fluorescence Measurements

Fluorescence emission spectra were recorded on a SPEX Fluorolog-2 spectrofluorometer (data interval of 0.5 nm, scan speed of 50 nm/min) supplied with DM-3000 software. Emission was measured in the ratio mode and corrected for the appropriate solvent-blanks, as well as for the wavelength-dependent bias of the optics and detection system. Fluorescence quantum yields of the protein, ϕ_{prot}, were determined by comparison with a standard,[36] namely, an aqueous solution of twice-recrystallized N-acetyltryptophanamide with $\phi_{stan} = 0.14$:[37]

$$\phi_{prot} = \phi_{stan} \frac{F_{prot}}{F_{stan}} \frac{D_{stan}}{D_{prot}} \qquad (2)$$

Here the absorption is denoted as D and F is the fluorescence intensity integrated over the range of 300–450 nm. Measurements were carried out with excitation at 295 nm. Since the Trp quantum yield may be evaluated by the steady-state method only with limited accuracy, we made similar estimates by fluorescence lifetime measurements, which have the advantage of being independent of concentration. The difference in quantum yield values recovered by both methods was below 10%.

Direct Energy Transfer Data Analysis

The direct energy transfer efficiency E was calculated as the relative loss of donor fluorescence due to interaction with the acceptor:[38,39]

$$E = 1 - \frac{\phi_{D,A}}{\phi_D} \qquad (3)$$

Here, ϕ_D and $\phi_{D,A}$ are the fluorescence quantum yields of the donor in the absence and presence of the acceptor, respectively. Further, the energy transfer efficiency is directly related to the donor–acceptor distance R_{DA} and the characteristic donor–acceptor distance R_o:

TABLE I. Structural Characteristics of Apomyoglobin in Different Conformational States

System	Conformation	Experimental conditions	$-[\Theta]_{222} \times 10^3$ (deg · cm^2 · dmol^{-1})	V_{mol}[a]	$\langle R_{AH} \rangle$ Å	$\langle R_{AG} \rangle$ Å
Holomyoglobin	Globular[b]	pH (6.5–7.5)	21–24	—	22	24
Native	Globular	pH (6.5–7.5)	17–23	1	22	24
Molten globule	Globular[b]	pH 4.2	10–11.5	1.7[c]	22	27
Intermediate	Coil-like	pH 2, 500 mM KCl	10	—	24	28
Intermediate	Coil-like	pH 2, 50 mM Na_2SO_4	10	4.3	24	28
Unfolded	Coil-like	pH 2	3.5–4	6.5	>50	>50

[a]Relative molecular volume.
[b]As reported in references.[14,41]
[c]As reported in references.[41,48,49]

$$E = \frac{1}{1 + \left(\frac{R_{DA}}{R_o}\right)^6} \quad (4)$$

The latter quantity is given by the well-known equation:[38]

$$R_o^6 = \frac{9000 \ln 10}{128\pi^5 N} \frac{\langle k^2 \rangle \phi_D}{n^4} \int_0^\infty F_D(\lambda)\varepsilon_A(\lambda)\lambda^4 d\lambda \quad (5)$$

where the parameter ϕ_D is as defined above, n is the refractive index of the medium, N is Avogadro's number, and λ is the wavelength. $F_D(\lambda)$ is the fluorescence spectrum of the donor with the total area normalized to unity, and $\varepsilon_A(\lambda)$ is the molar extinction coefficient of the acceptor. These data were obtained directly from independent experiments on each conformational state of interest. The $\langle k^2 \rangle$ represents the effect of the relative orientations of the donor and acceptor transition dipoles on the energy transfer efficiency. For a particular donor–acceptor orientation this parameter is given as:

$$k = (\cos\alpha - 3\cos\beta\cos\gamma) \quad (6)$$

where α is the angle between the transition moments of the donor and the acceptor, and β and γ are the angles between the donor and acceptor transition moments and the donor–acceptor vector, respectively. In an unfolded protein, a large number of random donor–acceptor orientations are possible, resulting in $\langle k^2 \rangle = 0.67$ as a statistical average.[38,40] In native and molten globules of apoMb, $\langle k^2 \rangle$ was found[20] to be 0.18. The latter was used to analyze the data obtained for anion-induced states, which exhibited similar helicity to the molten globules at pH 4.2 (see Table I). Since R_o depends on $\langle k^2 \rangle^{1/6}$, i.e., it is a very smooth function, the uncertainty associated with this assumption should be small for $\langle k^2 \rangle$ varying from 0.18 (native) to 0.67 (unfolded). Altogether, R_o values calculated for native and molten globules had values of 22 Å and 24 Å, respectively. For acid-unfolded and anion-induced forms, the values of 28 Å and 26 Å were obtained. Regarding the macromolecular conformations, note, that energy transfer experiments report the reciprocal of donor–acceptor distance, $\langle 1/R_{DA} \rangle$. This parameter of the conformational ensemble is most influenced by the more compact macromolecular species.

Modification of Apomyoglobin for Energy Transfer Experiments

Tyrosine residues were modified by reaction with tetranitromethane essentially as described.[20] The reaction with native protein allows for selective nitration of Tyr146, whereas the reaction with unfolded protein produces a fully modified sample with nitration of both Tyr103 and Tyr146. The selectivity of modification was estimated by amino acid analysis; only fragments containing Tyr103 or Tyr146 showed the increase of 45 a.u., the mass of the NO_2 group. The extent of modification was assessed by both spectrophotometry and mass spectroscopy. Specifically, the molar excess of nitro-Tyr per protein molecule was calculated[26] with $\epsilon_{381nm} = 2{,}200\ M^{-1} \cdot cm^{-1}$. In addition, the mass of horse apoMb was found to be 1,6951 a.u., and that of selectively and fully modified samples showed a shift of 45 or 90 a.u., respectively. Both techniques revealed the efficiency of modification to be about 95%.

RESULTS

Anion-Induced Refolding of Acid-Unfolded Apomyoglobin

Fluorescence and far-UV CD spectra were recorded for apoMb in different conformational states. This includes the native, molten globule, and unfolded states as well as partially folded forms stabilized at pH 2 by the presence of KCl or Na_2SO_4. Fluorescence measurements were carried out on selectively modified samples containing nitro-Tyr146, whereas in CD experiments unmodified protein was used.

Figure 2(A) illustrates the changes in the Trp fluorescence caused by the addition of the sulfate anion to the acid-unfolded protein solution. The spectrum recorded for native protein (circles) is also shown for comparison. Both the decrease in fluorescence intensity and an essential shift of the spectrum towards shorter wavelengths are observed over the range of 0–50 mM Na_2SO_4 with no further changes. Note that the fluorescence quantum yields of the unmodified proteins either in the native or acid-unfolded states are close to one another.[20] Quenching of Trp fluorescence in selectively modified samples indicates an increasing population of conformations where the Trp residues (donors) are closer to the nitro-Tyr146 (acceptors). Thus, fluorescence data testify to the collapse of the acid-unfolded apoMb chain induced by the presence of the

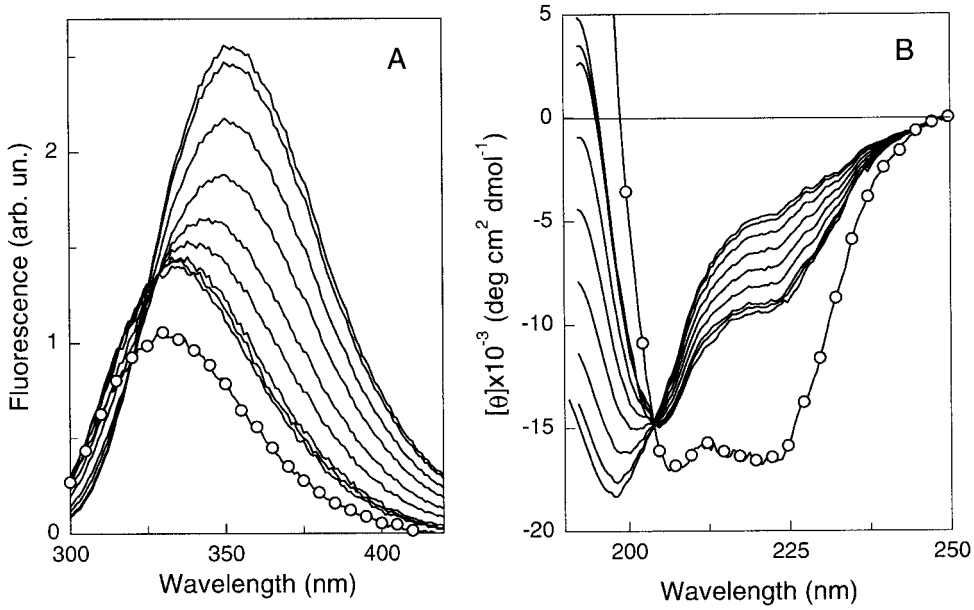

Fig. 2. Fluorescence (**A**) and far-UV circular dichroism (**B**) spectra of acid-unfolded apomyoglobin (pH 2, 23°C) for varying Na_2SO_4 concentrations (top-to-bottom): 0; 6; 11; 18; 24; 35; 53; 83; 175 mM. The spectra of native apomyoglobin (circles) are also shown for comparison. Fluorescence measurements (excitation wavelength of 295 nm) were carried out on selectively modified sample containing nitro-Tyr146, whereas in CD experiments unmodified protein was used. Other conditions were as described in Materials and Methods.

anion. A comparison of the fluorescence of native protein and that of the sulfate-induced state (pH 2, 50 mM Na_2SO_4) highlights some differences that might relate to the differences in the 3D-structures of these states. In particular, Trp fluorescence in the sulfate-induced state is about 1.5-times stronger than that in native protein, indicating less compactness of the protein molecule. In addition, the position of the spectrum maximum is red-shifted by ~6 nm, showing that Trp residues are more exposed to the solvent. The changes in the far-UV CD spectra of acid-unfolded apoMb with increasing sulfate concentration are shown in Figure 2(B) together with the spectrum recorded for native protein (circles). In fact, the CD data monitor the increasing propensity for the formation of secondary structure by the acid-unfolded apoMb chain. Structural transformations appear to be completed in 50 mM Na_2SO_4, since a further increase in anion concentration leads to no changes in the CD spectrum. Overall, CD data show that acid-unfolded apoMb restores about 50% of the native signal in the presence of 50 mM Na_2SO_4.

Figure 3 summarizes parameters monitored by fluorescence and circular dichroism, demonstrating that different intrinsic probes yield overlapping transitions. In addition, isosbestic points are observed in both sets of experiments [see Fig. 2(A, B)]. Given the above similarity, it seems most likely that the anion-refolding of pH-denatured apoMb is a two-stage process. Quite similar data were obtained for the refolding of apoMb induced by KCl. As an example, the far-UV CD spectrum of the chloride-induced state (pH 2, 500 mM KCl) is shown in Figure 4 together with that of the native (pH 7.5), acid-unfolded (pH 2), and sulfate-induced (pH 2, 50 mM Na_2SO_4) states. Note that the CD spectra of anion-induced states are indistinguishable, owing to the identity of the secondary structures induced.

Molecular Dimensions of the Anion-Induced Forms

Significant information as to the structure of anion-induced forms of apoMb is provided by small-angle X-ray scattering experiments. In particular, SAXS yields the radius of gyration, R_g, the most unambiguous measure of molecular compactness. The Guinier plot (see eq 1), however, may be complicated by the aggregation of the scattering particles. For instance, the aggregation of partially folded forms stabilized by 500 mM KCl at pH 2 makes quantitative analysis of SAXS data impossible for protein concentrations above 60 mM.[14] The sulfate-induced forms show no tendency for aggregation; therefore, we analyzed sulfate- rather than chloride-induced intermediates together with native and unfolded proteins. In addition, we exclusively use an extremely low protein concentration of 5 mM. The Guinier plots generated for the native (pH 7.5), acid-unfolded (pH 2), and sulfate-induced (pH 2, 50 mM Na_2SO_4) states of apoMb are shown in Figure 5. All samples exhibit a linear dependence at small angles, testifying to the relative homogeneity of each sample. Larger particles exhibit steeper slopes. Fitting the SAXS data to eq 1 yields R_g values of 19 Å and 35 Å for the native and acid-unfolded states, respectively. These R_g estimates correspond well to those previously reported.[14,41] For the sulfate-induced state, the R_g value of 29 Å was obtained.

Further information, provided by SAXS experiments, relates to the density of protein molecules. Specifically, the Kratky plot, $I(q) \cdot q^2$ vs. q, is known to be a sensitive indicator of protein conformation.[34,42–45] For instance, Kratky plots for globular proteins exhibit a characteristic

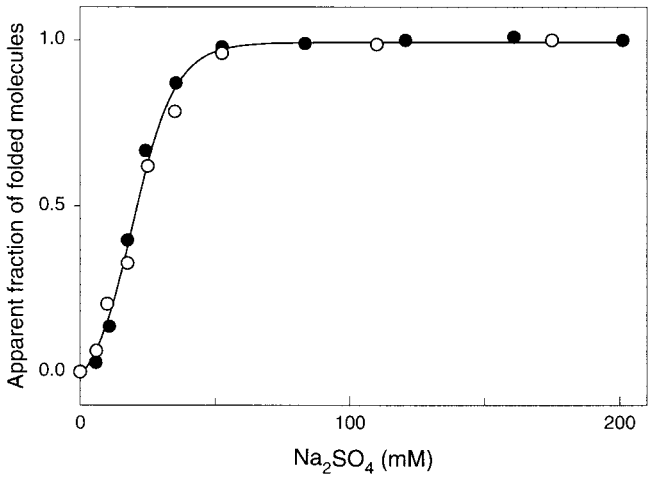

Fig. 3. Equilibrium Na_2SO_4-refolding curves for acid-unfolded apomyoglobin (pH 2, 23°C). The conformational transition was followed by ellipticity at 222 nm (solid circles) and the intrinsic fluorescence excited at 295 nm (open circles). Raw data were converted to the fraction of folded molecules, f, assuming the two-state model and plotted against Na_2SO_4 concentration. The solid lines are the non-linear least squares fits of the data to the equation $\frac{f}{1-f} = \exp\left(-\frac{\Delta G}{RT}\right)$

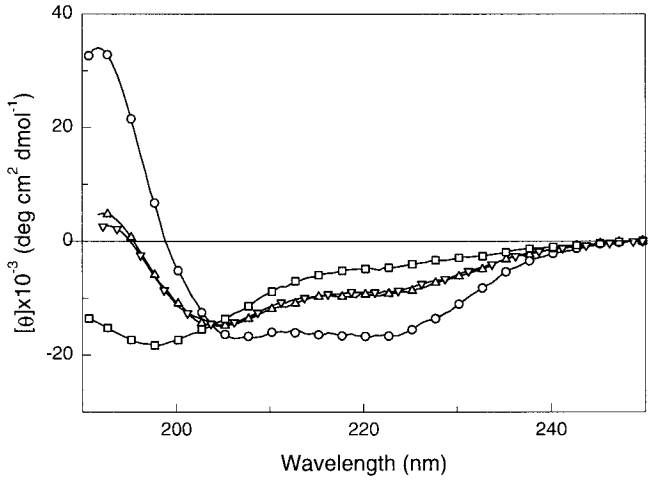

Fig. 4. Far-UV CD spectra of the native apomyoglobin at pH 7.5 (circles), acid-unfolded apomyoglobin at pH 2 (squares), and that in chloride-induced state at pH 2 and 500 mM KCl (upward triangles) and in sulfate-induced state at pH 2 and 50 mM Na_2SO_4 (downward triangles). Other conditions were as described in Materials and Methods.

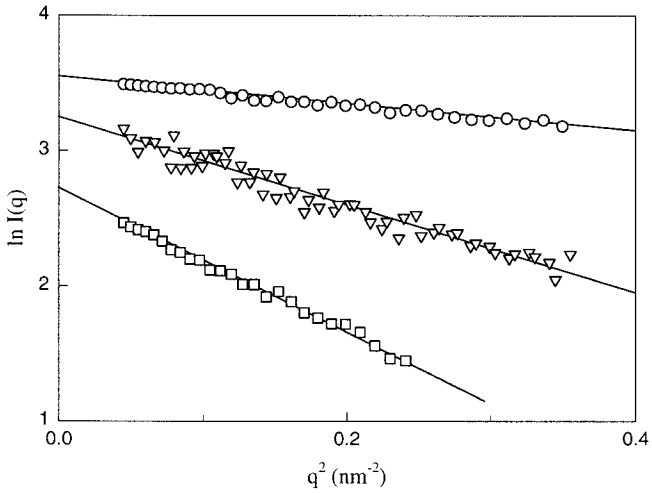

Fig. 5. Guinier plots of X-ray scattering data for native apomyoglobin at pH 7.5 (circles), acid-unfolded apomyoglobin at pH 2 (squares), and the sulfate-induced state at pH 2 and 50 mM Na_2SO_4 (triangles). For clarity, each plot is shifted along the *ln I(q)* axis. The protein concentration was 5 μM. Other conditions were as described in Materials and Methods.

maximum with the position depending on the molecular size: Larger particles exhibit a maximum at smaller angles. By contrast, unfolded proteins scatter X-rays as random coils and show no maximum on the Kratky plot. The Kratky plots generated for apoMb in different conformational states are shown in Figure 6. A large difference in the shapes of the scattering curves is clearly visible. In fact, these data indicate that native apoMb is a globular particle, whereas no globular structures were observed in either the acid-unfolded or the sulfate-induced states. Altogether, it appears that the sulfate-induced form of apoMb is a partially collapsed molecule (fluorescence, SAXS) with developed secondary structure (CD) and with low packing density of monomer units (SAXS). Quite similar structural characteristics have recently been revealed for the least ordered anion-induced conformation of staphylococcal nuclease,[4] and for the pH-induced and/or Zn^{2+}-induced partially folded conformations of the "natively unfolded" human prothymosin a.[46,47]

AGH-Core in Anion-Induced Forms

In order to provide some clues as to the 3D-structures of the anion-induced states of apoMb, we performed fluorescence energy transfer experiments. In particular, we measure the apoMb fluorescence and calculate by eq 3 the energy transfer efficiency induced by the acceptors located at position 103 and 146. The energy transfer in selectively modified samples reflects the interactions of Trp residues with nitro-Tyr146 whereas that in fully modified samples

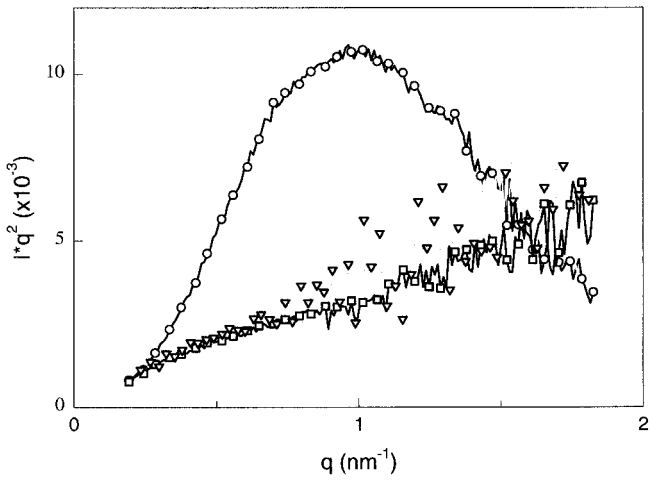

Fig. 6. Kratky plots of scattering curves from the native apomyoglobin at pH 7.5 (circles), acid-unfolded apomyoglobin at pH 2 (squares), and that in sulfate-induced state at pH 2 and 50 mM Na_2SO_4 (triangles). The conditions are the same as in Figure 5.

monitors the interactions of Trp residues with both nitrated Tyr residues. Given the additive character of the energy transfer we calculate the efficiency for each acceptor as follows:

$$E_{146} = E_{\text{selectively}} \quad (7)$$

$$E_{103} = E_{\text{fully}} - E_{\text{selectively}} \quad (8)$$

As expected, in unfolded molecules the Trp fluorescence is only slightly affected by the presence of the nitro-Tyr, either in selectively or fully modified samples. For example, the energy transfer efficiency in the fully modified sample was found to be about 8%, similar to that reported previously.[20] These data indicate that the average distance from (Trp7-Trp14) to Tyr146 and to Tyr103 in the acid-unfolded protein is about 50 Å (Table I). In anion-induced forms, the observed efficiencies of 60 and 30% are associated with the correspondent AH and AG dimensions of 24 Å and 28 Å, respectively. These values are very close to that of the native and molten globule states of apoMb, and to the corresponding molecular dimensions in horse myoglobin (Table I). In addition, very similar values for AH and AG dimensions were obtained in our previous studies[28] of the nonnative forms of apoMb stabilized by NaTCA, NaTFA, $NaClO_4$. Thus, the linear dimensions of the AGH core in all nonnative states of apoMb studied so far coincide and are very close to those of holomyoglobin.

DISCUSSION

The structural transformations of acid-unfolded proteins induced by the presence of anions have been intensively investigated over the last decade.[22–25] Although the molecular mechanism of this phenomenon is still unclear, three principal means through which anions can induce the folding of proteins can be suggested: First, anions can provoke folding through a general ionic strength effect, i.e., by a shielding of the electrostatic repulsions among the positively charged residues in unfolded chains. Second, the mechanism might include a Hofmeister effect, i.e., stabilization of native proteins through the anion's ability to alter the structure of water. Third, anions can induce refolding by favorable specific binding to the folded conformation, thereby shifting the equilibrium towards the native state.

Regarding the molecular structures of anion-induced forms, the present study reveals that the nonnative forms of apoMb induced by KCl or Na_2SO_4 exhibit a significant amount of secondary structure (circular dichroism), low packing density of protein molecule (SAXS), and the native-like dimensions of the AGH core (fluorescence energy transfer). In fact, the distances between the aromatic residues residing in the A-, H-, and G- fragments are very close to those in native myoglobin. The density of the protein molecule, however, is similar to that in the unfolded state, exhibiting characteristics of a fluctuating coil. It appears that both sulfate- and chloride-induced states can be identified as compact denatured states, comprising a native-like core with partially buried hydrophobic residues. These results suggest the native-like tertiary fold of the polypeptide chain is present, i.e., the spatial organization of secondary structure elements emerges prior to the formation even of the MG state.

At this juncture, some comments about protein denaturation are appropriate. Protein unfolding, being an abrupt cooperative increase of protein volume and the cooperative destruction of protein secondary structure, is usually observed upon a change of temperature or solvent composition, and results in loss of biochemical activity. The most reasonable model of protein denaturation has been suggested in the theory of coil–globule transitions,[50] where the protein unfolding was considered from the first principles of molecular physics, without referring to the specific properties of polypeptide chains. In fact, volume interactions were treated on a general physical basis, i.e., a "poor solvent" encourages the attraction of macromolecular segments and hence a chain has "to condense upon itself." In a "good solvent," repulsive forces act primarily between the segments and the macromolecule conforms to a loose fluctuating coil. The character of a globule–coil transition depends essentially on both the chain length and chain stiffness.[50] For flexible chains, it occurs smoothly being a second-order phase transition. For stiff chains, the transition is sharp and approaches a first-order phase transition. In general, protein unfolding is expected to occur in accordance with an "all-or-none" principle, or at least through a small number of discrete intermediate states, if the protein globule consists of parts having different stabilities. The theory also predicts that apart from "gas and liquid" (e.g., "coil and molten globule"), other diverse condensed states may appear in the system due to actual volume interactions. Therefore, phase transitions between different globular states (e.g, "native and molten globules"), as well as between any globular and coil states might occur.

The most unambiguous characteristic of the globular state remains the density of the macromolecule. Specifically, the density of a globule is expected to be independent

TABLE II. Hydrodynamic Characteristics of the Globular Proteins in Different Conformational States

Protein	*M* KDa	$\langle R_S \rangle$, Å ([η], ml/g)	References	Protein	*M* KDa	$\langle R_S \rangle$, Å ([η], ml/g)	References
Native state							
Basic protein[1]	4.3	(3.8)	54	RTEM β-Lactamase[2]	29.0	24.5	76
Immunoglobulin binding[2]	6.2	(2.8)	53	Ovalbumin A1[6]	36.0	(3.9)	56
Ubiquitin[3]	8.5	16	52	β-lactoglobulin[3]	36.8	(3.4)	60
(apo)Cytochrome C[4]	11.7	18.5	14, 41	Pepsinogen[5]	40.0	(3.2)	60
Ribonuclease A[3]	13.7	(3.4)	60	G-actin[11]	41.6	28	57
α-Lactalbumin[5]	14.1	18.5	52	(MMP-1) Interstitial collagenase[10]	42.6	27.2	74
Lysozyme[6]	14.2	(2.7)	51	Ovalbumin[6]	45.3	(4.4)	83
Intestinal fatty acid binding[5]	15.1	20	81	Serum albumin[3]	66.3	(3.7)	51
Tumor supressor, p16	16.5	20	80	α-fetoprotein[5]	66.5	32.4	66
(apo)Myoglobin[4]	17.0	20.9 (3.9)	14, 41	Hemoglobin	68.0	(3.6)	51
Staphylococcal nuclease[7]	17.5	20.5	4	Dnak[2]	70.0	32.5	67
β-Lactoglobulin[8]	18.5	22	78	Creatine kinase,[12] dimer	86.2	35.2	68
Sarcoplasmic calcium binding[9]	19.5	21.5	72	Purple acid phosphatase[13,18]	101	41.7	77
Adenylate kinase[10]	21.7	21.9	71	Acetylcholinesterase[14,18]	121	49	75
Ovine placental lactogen	21.8	22.4	73	Lactate dehydrogenase[19]	141	43.9	52
Trypsinogen[3]	25.4	19.8	82	GAP dehydrogenase[10,19]	145	(3.8)	62
Chymotrypsinogen[3]	25.7	(2.5)	60	Aldolase[19]	160	(4)	60
Tryptophan synthase[2,17]	28.7	24.2	69, 70	Phosphorybosil transferase[20]	210	51	52
β-Lactamase[7,11]	28.8	23.7	2, 52	Catalase	220	(4)	63
Carbonic anhydrase B[3]	28.8	23.3 (2.9)	3, 61	Bushy stunt virus, multimer	10,700	(3.4)	51
Molten globule state							
(apo)Cytochrome C[4]	11.7	20.1	41, 58	Trypsinogen[3]	25.4	25.6	82
α-Lactalbumin[5]	14.1	20.2	52	β-Lactamase[7,11]	28.8	26.6	2, 52
Tumor supressor, p16	16.5	23.6	80	Carbonic anhydrase B[3]	28.8	26.4	3
(apo)Myoglobin[4] (pH 4)	17.0	25.3 (4.1)	41, 48	RTEM β-lactamase[2]	28.9	27	76
β-Lactoglobulin[8]	18.5	24	78	(MMP-1) Interstitial collagenase[10]	42.6	32.1	74
Sarcoplasmic calcium binding[9]	19.5	24.2	72	Ovalbumin[6]	42.8	33.5 (5)	83, 88
Adenylate kinase[10]	21.7	24.3	71	α-Fetoprotein[5]	66.5	35.5	66
Ovine placental lactogen	21.8	24.5	73	Dnak[2]	69.0	36.3	67
Pre-molten globule state							
Intestinal fatty acid-binding[5]	15.1	29	81	β-Lactamase[7]	28.8	32.4	2
Tumor suppressor, p16	16.5	30.3	80	Carbonic anhydrase B[3]	28.8	31.7	3
Staphylococcal nuclease[7] (KCl)	16.8	29.2	present	(MMP-1) Interstitial collagenase[10]	42.6	40.2	74
(apo)Myoglobin[4] (Na_2SO_4)	17.0	27.2	present	Creatine kinase[12]	43.1	42	68
Adenylate kinase[10]	21.7	30.3	71	Dnak[2]	69.0	53.1	67
Tryptophan synthase[2,17]	28.7	33.9	69, 70				
Unfolded state (6 M GdnHCl, 25°C)							
Insulin[3]	3.0	(6.1)	60	Tryptophan synthase[2,17]	28.7	57	69, 70
Albebetin	7.8	24.1	86	β-Lactamase[7,11]	28.8	52	2, 52
Ubiquitin[3]	8.5	25.8	52	Carbonic anhydrase B[3]	28.8	52 (29.5)	3, 61
(apo)Cytochrome C[4]	11.7	34	58, 59	Phosphoribosyl transferase	35.0	(31.8)	85
Prothymosin α[5]	12.1	31.4	46, 47	Lactate dehydrogenase	35.3	55.1	52
Ribonuclease A[3]	13.7	32.8 (16.2)	60	Ovalbumin A1[6]	36.0	(31.1)	56
α-Lactalbumin[5]	14.1	31.8	52	GAP dehydrogenase[10]	36.3	(34.4)	62
Lysozyme[6]	14.2	(17)	84	Pepsinogen[5]	40.0	(31.4)	60
α-Synuclein[5]	14.5	34.3	present	Aldolase	40.0	(35.4)	60
Intestinal fatty acid-binding[5]	14.7	36.1	81	G-actin[12]	41.6	60	57
Intestinal fatty acid-binding[5]	15.1	36.4	81	Creatine kinase[12]	43.1	61	68
Myoglobin	17.2	(18.8)	87	Purple acid phosphatase[13]	50.2	72	77
Apoflavodoxin[15]	16.5	37.7	79	Serum albumin[3]	66.3	82 (52)	51, 66
Tumor suppressor, p16	16.5	37.1	80	α-Fetoprotein[5]	66.5	72	66
(apo)Myoglobin[4]	17.0	43	41, 58	Dnak[2]	69	73	67
Staphylococcal nuclease[7]	17.5	36	4	Transferrin	81	86.8	52
Dihydrofolate reductase[16]	17.6	37.6	65	Acetylcholinesterase[14]	121	110	75
β-Lactoglobulin[2,8]	18.5	37 (22.7)	78, 60	Thyroglobulin[3]	165	(81.6)	64
Adenylate kinase[10]	21.7	42.1	71	Myosin	197	(92.6)	87
Ovine placental lactogen	21.8	41.6	73	Cervical mucus plycoprotein	12,000	1300	55
Chimotrypsinogen[3]	25.7	(26.8)	60				

[1]Marine turtle (white egg); [2]*E. coli;* [3]bovine; [4]horse; [5]human; [6]chicken; [7]*S. aureus;* [8]equine; [9]nereis; [10]porcine; [11]*B. cereus;* [12]rabbit; [13]red kidney bean; [14]electric ray; [15]fragment; [16]circularly permuted; [17]α-subunit; [18]dimerized; [19]tetramer; [20]hexamer.

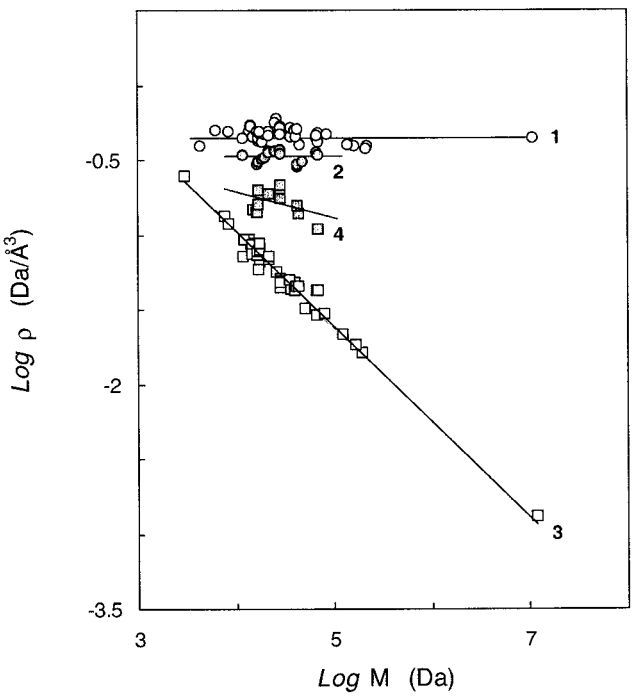

Fig. 7. Variation of the density of protein molecules ρ with protein molecular weight M for native (**1**), molten globule (**2**), 6M GdnHCl-unfolded (**3**), and the compact denatured (**4**) conformational states. The data used are summarized in Table II.

of chain length.[50] By contrast, the density of partially collapsed or swelled macromolecules depends on both the chain length, and therefore on its molecular weight M, and on the solvent. For instance, under conditions known as "ideal", i.e., when the attractions of the macromolecular segments are balanced by those with the solvent, the density of macromolecules follows $M^{-0.5}$. It appears that understanding protein folding might be aided by an analysis of the density of proteins adopting different conformational states. In Table II, we summarize the structural data obtained for a variety of proteins by different hydrodynamic techniques. In this regard, gel filtration and dynamic light scattering experiments provide a measure of the hydrodynamic Stokes' radius of macromolecules in solution, R_s, and allow estimating the apparent molecular density ρ for the equivalent hydrodynamic R_s-sphere, $\rho_s = M/\left(\frac{4}{3}\pi R_S^3\right)$. The intrinsic viscosity of a protein solution, [η], yields directly the specific volume and/or the apparent density of the protein molecules as $\rho = \upsilon N/[\eta]$. Since hydrodynamic data are sensitive to the shape of macromolecules, the proteins exhibiting a nearly spherical shape were chosen for analysis. The asymmetry of native molecules was estimated from NMR and X-ray crystallography data, calculating three principal axes of gyration and further the shape factor ν.[51]

The logarithmic plot in Figure 7 displays molecular density as a function of the molecular weight for over 100 proteins in the native, molten globule, and fully unfolded states, as well as in the compact denatured or pre-molten globule states. Overall, four equilibrium conformations characterized by essential differences in molecular density and its dependence on the peptide length are clearly visible. For instance, analysis of the measured hydrodynamic radii (Table II) for native proteins, known from structural studies to be essentially spherical, indicates that there is a strong correlation between the molecular dimensions and the chain length. Specifically, in native globules molecular density shows no changes with the chain length, giving a constant value of about 0.5 Da/Å (curve 1). These data agree well with those reported previously.[89] Molten globules also exhibit a lack of molecular weight dependence, but have a lower density of 0.39 Da/Å (curve 2). For characterizing the unfolded states, we have concentrated on proteins without crosslinks (i.e., on proteins either with reduced disulfide bridges or without cysteines), as the presence of these might perturb significantly the molecular dimensions. Further, only strongly denaturing conditions (6 M GdnHCl) were considered, in which the proteins were shown to be fully unfolded. As can be appreciated, a correlation is also observed for unfolded proteins, and the apparent density follows the molecular weight as $\rho \sim M^{-0.64}$ indicating relatively good solvent conditions (curve 3). Quite similar results, i.e., $\rho \sim M^{-0.66}$, have been reported in previous studies of protein denaturation.[87,89] The data generated for the "pre-molten globule" and "compact denatured" states are combined into one curve, demonstrating intermediate behavior (curve 4). In fact, these data correspond to poor solvent conditions, where some intramolecular interactions occur, compared to the fully unfolded state in 6 M GdnHCl. In this regard, we exclusively used proteins exhibiting four-state GdnHCl-induced unfolding with molten and pre-molten globule states along with native and unfolded states. Overall, given the observed correlations, it appears that the compact denatured state might be a general intermediate in protein folding along with the native, molten globule, and fully unfolded conformations. As to the partially folded forms of apoMb stabilized by KCl and/or Na_2SO_4, we find that their apparent densities estimated by means of gel filtration experiments superimpose perfectly onto curve 4, thus exhibiting the features of the compact denatured state.

A protein's unfolded state is usually considered to be a molecular distribution over conformational substates with varying degrees of residual structure. Clearly, in a good solvent, it would shift toward states with less residual structure and eventually to the completely unfolded state. In a poor solvent, the distribution is expected to be centered around rather compact substates with significant residual structure. Which unfolded ensemble has any biological relevance remains a serious question. It might well be the case that the collapsed conformational state with fluctuating density, comprised of a specific "native-like" core with burial of hydrophobic residues, is a key feature of protein folding. The existence of such a state substantially reduces any search through conformational space, ensuring rapid folding. In addition, formation of the topology of a hydrophobic core may be an essential precursor for achieving the unique fold of a protein.

ACKNOWLEDGMENTS

We thank Ian Millett, Daniel Segel and Sebastian Doniach for help with SAXS measurements. We express our gratitude to Robert Jernigan for carefully reading the manuscript and valuable discussion, and to Jay R. Knutson and Anthony L. Fink for use of their equipment.

REFERENCES

1. Ptitsyn OB. Molten globule and protein folding. Adv Protein Chem 1995;47:83–229.
2. Uversky VN, Ptitsyn OB. "Partly folded" state, a new equilibrium state of protein molecules: four-state guanidinium chloride-induced unfolding of beta-lactamase at low temperature. Biochemistry 1994;33:2782–2791.
3. Uversky VN, Ptitsyn OB. Further evidence on the equilibrium "pre-molten globule state": four-state guanidinium chloride-induced unfolding of carbonic anhydrase B at low temperature. J Mol Biol 1996;255:215–228.
4. Uversky VN, Karnoup AS, Segel D, Seshadri S, Doniach S, Fink AL. Anion-induced folding of Staphylococcal nuclease: characterization of multiple equilibrium partially folded intermediates. J Mol Biol 1998;278:879–894.
5. Kuwajima K. The molten globule state as a clue for understanding the folding and cooperativity of globular-protein structure. Proteins Struct Funct Genet 1989;6:87–103.
6. Baldwin RL. Molten globule: specific or non-specific folding intermediate? Chemtracts Biochem Mol Biol 1991;2:379–389.
7. Christensen H, Pain RH. Molten globule intermediates and protein folding. Eur Biophys J 1991;19:221–229.
8. Dobson CM. Unfolded proteins, compact states and molten globules. Curr Opin Struct Biol 1992;2:6–12.
9. Fink AL. Molten globules. Meth Mol Biol 1995;40:343–360.
10. Hughson FM, Wright PE, Baldwin RL. Structural characterization of a partly folded apomyoglobin intermediate. Science 1990; 249:1544–1548.
11. Lecomte JTJ, Sukits SF, Bhattacharya S, Falzone C. Conformational properties of native sperm whale apomyoglobin in solution. Protein Sci 1999;8:1484–1491.
12. Cocco MJ, Lecomte JT. Characterization of hydrophobic cores in apomyoglobin: a proton NMR spectroscopy study. Biochemistry 1990;29:11067–11072.
13. Evans SV, Brayer GD. High-resolution study of the three-dimensional structure of horse heart metmyoglobin. J Mol Biol 1990;213:885–897.
14. Kataoka M, Nishii I, Fujisawa T, Ueki T, Tokunaga F, Goto Y. Structural characterization of the molten globule and native states of apomyoglobin by solution X-ray scattering. J Mol Biol 1995;249:215–228.
15. Barrick D, Baldwin RL. The molten globule intermediate of apomyoglobin and the process of protein folding. Prot Sci 1993;2: 869–876.
16. Goto Y, Fink AL. Phase diagram for acidic conformational states of apomyoglobin. J Mol Biol 1990;214:803–805.
17. Barrick D, Baldwin RL. Three-state analysis of sperm whale apomyoglobin folding. Biochemistry 1993;32:3790–3796.
18. Jennings PA, Wright PE. Formation of a molten globule intermediate early in the kinetic folding pathway of apomyoglobin. Science 1993;262:892–896.
19. Eliezer D, Yao J, Dyson HJ, Wright PE. Structural and dynamic characterization of partially folded states of apomyoglobin and implications for protein folding. Nat Struct Biol 1998;5:148–155.
20. Tcherkasskaya O, Ptitsyn OB. Direct energy transfer to study the 3D structure of non-native proteins: AGH complex in molten globule state of apomyoglobin. Protein Eng 1999;12:485–490.
21. Tcherkasskaya O, Ptitsyn OB, Knutson JR. Nanosecond dynamics of tryptophans in different conformational states of apomyoglobin proteins. Biochemistry 2000;39:1879–1889.
22. Goto Y, Takahashi N, Fink AL. Mechanism of acid-induced folding of proteins. Biochemistry 1990;29:3480–3488.
23. Fink AL, Oberg KA, Seshadri S. Discrete intermediates vs. molten globule models of protein folding: characterization of partially-folded intermediates of apomyoglobin. Folding Des 1997;3:19–25.
24. Loh SN, Kay MS, Baldwin RL. Structure and stability of a second molten globule intermediate in the apomyoglobin folding pathway. Proc Natl Acad Sci USA 1995;92:5446–5450.
25. Nishii I, Kataoka M, Goto Y. Thermodynamic stability of the molen globule states of apomyoglobin. J Mol Biol 1995;250:223–238.
26. Lundblad RL. Chemical reagents for protein modification. Boca Raton: CRC Press; 1991. 345p.
27. Rischel C, Poulsen FM. Modification of a specific tyrosine enables tracing of the end-to-end distance during apomyoglobin folding. FEBS Lett 1995;374:105–109.
28. Tcherkasskaya O, Ptitsyn OB. Molten globule versus variety of intermediates: influence of anions on pH-denatured apomyoglobin. FEBS Lett 1999;455:325–331.
29. Teale FWJ. Cleavage of the haem-protein link by acid methylethylketone. Biochim Biophys Acta 1959;35:543.
30. Laemmli UK. Cleavage of structural proteins during the assembly of the head of bacteriophage T4. Nature 1970;227:680–685.
31. Gill SC, von Hippel PH. Calculation of protein extinction coefficients from amino acid sequence data. Anal Biochem 1989;182: 319–326.
32. Wakatsuki S, Hodgson KO, Eliezer D, Rice M, Hubbard S, Gillis N, Doniach S. Small-angle X-ray-scattering diffraction system for studies of biological and other materials at the Stanford-Synchrotron-Radiation-Laboratory. Rev Sci Instrum 1992;63: 1736–1740.
33. Tsuruta H, Brennan S, Rek ZU, Irving TC, Tompkins WH, Hodgson KO. A wide-bandpass multilayer monochromator for biological small-angle scattering and fiber diffraction studies. J Appl Cryst 1998;31:672–682.
34. Glatter O, Kratky O. Small angle X-ray scattering. New York: Academic Press; 1982. 515p.
35. Woody RW. Theory of circular dichroism of proteins. In: Fasman GD, editor. Circular dichroism and the conformational analysis of biomolecules. New York: Plenum Press; 1996. p 25–69.
36. Parker CA, Rees WT. Corrections of fluorescence spectra and the measurement of fluorescence quantum efficiency. Analyst 1960;85: 587–600.
37. Eisinger M. A variable temperature, UV luminescence spectrograph for small samples. J Photochem Photobiol 1969;9:247–258.
38. Förster T. Intermolecular energy migration and fluorescence. Ann Physik 1948;2:55–75.
39. Lakowicz JR. Principles of fluorescence spectroscopy. New York: Kluwer Academic/Plenum; 1999. 698p.
40. Blumen A. On the anisotropic energy-transfer to random acceptors. J Chem Phys 1980;74:6926–6933.
41. Gast H, Damaschun H, Misselwitz R, Müller-Frohne M, Zirwer D, Damaschun G. Compactness of protein molten globules: temperature-induced structural changes of the apomyoglobin folding intermediate. Eur Biophys J 1994;23:297–305.
42. Kataoka M, Hagihara Y, Mihara K, Goto Y. Molten globule of cytochrome c studied by small angle X-ray scattering. J Mol Biol 1993;229:591–596.
43. Eliezer D, Chiba K, Tsuruta H, Doniach S, Hodgson KO, Kihara H. Evidence of an associative intermediate on the myoglobin folding pathway. Biophys J 1993;65:912–917.
44. Semisotnov GV, Kihara H, Kotova NV, Kimura K, Amemiya Y, Wakabayashi K, Serdyuk IN, Timchenko AA, Chiba K, Nikaido K, Ikura T, Kuwajima K. Protein globularization during folding. A study by synchrotron small-angle X-ray scattering. J Mol Biol 1996;262:559–574.
45. Doniach S, Bascle J, Garel T, Orland H. Partially folded states of proteins: characterization by X-ray scattering. J Mol Biol 1995;254: 960–967.
46. Uversky VN, Gillespie JR, Millett IS, Khodyakova AV, Vasiliev AM, Chernovskaya TV, Vasilenko RN, Kozlovskaya GD, Dolgikh DA, Doniach S, Fink AL, Abramov VM. "Natively unfolded" human prothymosin α adopts partially-folded conformation at acidic pH. Biochemistry 1999;38:15009–15016.
47. Uversky VN, Gillespie JR, Millett IS, Khodyakova AV, Vasilenko RN, Vasiliev AM, Rodionov IL, Kozlovskaya GD, Dolgikh DA, Doniach S, Fink AL, Permyakov EA, Abramov VM. Zn^{2+}-mediated structure formation and compaction of the "natively unfolded" human prothymosin α. Biochem Biophys Res Commun 2000;267:663–668.
48. Griko YuV, Privalov PL, Venyaminov SYu, Kutyshenko VP. Thermodynamic study of the apomyoglobin structure. J Mol Biol 1988;202:127–138.

49. Eliezer D, Jennings PA, Wright PE, Doniach S, Hodgson KO, Tsuruta H. The radius of gyration of an apomyoglobin folding intermediate. Science 1995;270:487–488.
50. Grossberg AYu, Khohlov AR. Statistical physics of macromolecules. Moscow: Nauka; 1989. 344p.
51. Cantor CR, Schimmel PR. Biophysical Chemistry. New York: W. H. Freeman Company; 1980. p 561–665.
52. Uversky VN. Use of fast protein size-exclusion liquid chromatography to study the unfolding of proteins which denature through the molten globule. Biochemistry 1993;32:13288–13298.
53. Tcherkasskaya O, Knutson JR, Bowley SA, Frank MK, Gronenborn AM. Nanosecond dynamics of the single tryptophan reveals multi-state equilibrium unfolding of protein GB1. Biochemistry 2000;39:11216–11226.
54. Chakrabarti S, Sen PC, Sinha NK. Purification and characterization of a low molecular weight basic protein from marine turtle egg white. Arch Biochem Biophys 1988;262:286–292.
55. Sheehan JK, Carlstedt I. Hydrodynamic properties of human cervical-mucus glycoproteins in 6M-guanidinium chloride. Biochem J 1984;217:93–101.
56. Ahmad F, Salahuddin A. Reversible unfolding of the major fraction of ovalbumin by guanidine hydrochloride. Biochemistry 1976;15:5168–5175.
57. Kuznetsova IM, Biktashev AG, Khaitlina SY, Vassilenko KS, Turoverov KK, Uversky VN. Effect of self-association on the structural organization of partially folded proteins: inactivated actin. Biophys J 1999;77:2788–2800.
58. Goto Y, Calciano LJ, Fink AL. Acid-induced folding of proteins. Proc Natl Acad Sci USA 1990;87:573–577.
59. Hamada D, Hoshino M, Kataoka M, Fink AL, Goto Y. Intermediate conformational states of apocytochrome c. Biochemistry 1993; 32:10351–10358.
60. Tanford C, Kawahara K, Lapanje S, Hooker TM, Zarlengo MH, Salahuddin A, Aune KC, Takagi T. Proteins as random coils. 3. Optical rotatory dispersion in 6 M guanidine hydrochloride. J Am Chem Soc 1967;89:5023–5029.
61. Wong KP, Tanford C. Denaturation of bovine carbonic anhydrase B by guanidine hydrochloride. A process involving separable sequential conformational transitions. J Biol Chem 1973;248:8518–8523.
62. Harrington WF, Karr GM. Subunit structure of glyceraldehyde-3-phosphate dehydrogenase. J Mol Biol 1965;13:885–893.
63. le Maire M, Rivas E, Moller JV. Use of gel chromatography for determination of size and molecular weight of proteins: further caution. Anal Biochem 1980;102:12–21.
64. De Crombrugghe B, Pitt-Rivers R, Edelhoch H. The properties of thyroglobulin. XI. The reduction of the disulfide bonds. J Biol Chem 1966;241:2766–2773.
65. Uversky VN, Kutyshenko VP, Protasova NYu, Rogov VV, Vassilenko KS, Gudkov AT. Circularly permuted dihydrofolate reductase possesses all the properties of the molten globule state, but can resume functional tertiary structure by interaction with its ligands. Protein Sci 1996;5:1844–1851.
66. Uversky VN, Narizhneva NV, Ivanova TV, Tomashevski AYu. Rigidity of human a-fetoprotein tertiary structure is under the ligand control. Biochemistry 1997;36:13638–13645.
67. Palleros DR, Shi L, Reid KL, Fink AL. Three-state denaturation of DnaK induced by guanidine hydrochloride. Evidence for an expandable intermediate. Biochemistry 1993;32:4214–4221.
68. Clottes E, Leydier C, Couthon F, Marcillat O, Vial C. Denaturation by guanidinium chloride of dimeric MM-creatine kinase and its proteinase K-nicked form: evidence for a multiple-step process. Biochim Biophys Acta 1997;1338:37–46.
69. Gualfetti PJ, Iwakura M, Lee JC, Kihara H, Bilsel O, Zitzewitz JA, Matthews CR. Apparent radii of the native, stable intermediates and unfolded conformers of the alpha-subunit of tryptophan synthase from *E. coli*, a TIM barrel protein. Biochemistry 1999;38: 13367–13378.
70. Gualfetti PJ, Bilsel O, Matthews CR. The progressive development of structure and stability during the equilibrium folding of the alpha subunit of tryptophan synthase from Escherichia coli. Protein Sci 1999;8:1623–1635.
71. Zhang YL, Zhou JM, Tsou CL. Sequential unfolding of adenylate kinase during denaturation by guanidine hydrochloride. Biochim Biophys Acta 1996;1295:239–244.
72. Christova P, Cox JA, Craescu CT. Ion-induced conformational and stability changes in Nereis sarcoplasmic calcium binding protein: evidence that the APO state is a molten globule. Proteins 2000;40: 177–184.
73. Cymes GD, Grosman C, Delfino JM, Wolfenstein-Todel C. Detection and characterization of an ovine placental lactogen stable intermediate in the urea-induced unfolding process. Protein Sci 1996;5:2074–2079.
74. Zhang Y, Gray RD. Characterization of folded, intermediate, and unfolded states of recombinant human interstitial collagenase. J Biol Chem 1996;271:8015–8021.
75. Kreimer DI, Shin I, Shnyrov VL, Villar E, Silman I, Weiner L. Two partially unfolded states of *Torpedo californica* acetylcholinesterase. Protein Sci 1996;5:1852–1864.
76. Sarkar D, DasGupta C. Characterization of a molten globule intermediate during GdnHCl-induced unfolding of RTEM beta-lactamase from *Escherichia coli*. Biochim Biophys Acta 1996;12961: 85–94.
77. Cashikar AG, Rao NM. Role of the intersubunit disulfide bond in the unfolding pathway of dimeric red kidney bean purple acid phosphatase. Biochim Biophys Acta 1996;1296:76–84.
78. Ikeguchi M, Kato S, Shimizu A, Sugai S. Molten globule state of equine beta-lactoglobulin. Proteins 1997;27:567–575.
79. Maldonado S, Jiménez MA, Langdon GM, Sancho J. Cooperative stabilization of a molten globule apoflavodoxin fragment. Biochemistry 1998;37:10589–10596.
80. Tang KS, Guralnick BJ, Wang WK, Fersht AR, Itzhaki LS. Stability and folding of the tumour suppressor protein p16. J Mol Biol 1999;285:1869–1986.
81. Clerico EM, Peisajovich SG, Ceolin M, Ghiringhelli PD, Ermacora MR. Engineering a compact non-native state of intestinal fatty acid-binding protein. Biochim Biophys Acta 2000;1476:203–218.
82. Martins NF, Santoro MM. Partially folded intermediates during trypsinogen denaturation. Braz J Med Biol Res 1999;32:673–682.
83. Koseki T, Kitabatake N, Doi E. Conformational changes in ovalbumin at acid pH. J Biochem (Tokyo) 1988;103:425–430.
84. Tanford C. Protein denaturation. Adv Protein Chem 1968;23:122–282.
85. Voll MJ, Appella E, Martin RG. Purification and composition studies of phosphoribosyladenosine triphosphate:pyrophosphate phosphoribosyltransferase, the first enzyme of histidine biosynthesis. J Biol Chem 1967;242:1760–1767.
86. Aphasizheva IYu, Dolgikh DA, Abdullaev ZK, Uversky VN, Kirpichnikov MP, Ptitsyn OB. Can grafting of an octapeptide improve the structure of a de novo protein? FEBS Lett 1998;425: 101–104.
87. Tanford C, Kawahara K, Lapanje S. Proteins in 6 M guanidine hydrochloride. Demonstration of random coil behavior. J Am Chem Soc 1967;89:729–736.
88. Castellino FJ, Barker R. Examination of the dissociation of multichain proteins in guanidine hydrochloride by membrane osmometry. Biochemistry 1968;7:2207–2217.
89. Wilkins DK, Grimshaw SB, Receveur V, Dobson CM, Jones JA, Smith LJ. Hydrodynamic radii of native and denatured proteins measured by pulse field gradient NMR techniques. Biochemistry 1999; 38:16424–1631, and references therein.